Surface Science 620 (2014) 23–29

Contents lists available at ScienceDirect

Surface Science

journal homepage: www.elsevier.com/locate/susc

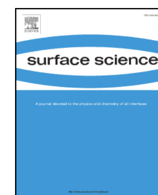

Self-organized trench–island structures in epitaxial cobalt silicide growth on Si(111)

J.C. Mahato, Debolina Das, R. Batabyal, Anupam Roy [1], B.N. Dev *

Department of Materials Science, Indian Association for the Cultivation of Science, 2A & 2B Raja S. C. Mullick Road, Jadavpur, Kolkata 700032, India

ARTICLE INFO

Article history:
Received 10 August 2013
Accepted 7 October 2013
Available online 12 October 2013

Keywords:
Nanoscale materials and structures
Scanning tunneling microscopy
Surface structures
Epitaxial silicide and trench

ABSTRACT

Sub-monolayer Co deposition on clean Si(111)–(7 × 7) surfaces has been found to form nanoscale $CoSi_2$ islands with a surrounding trench of one Si bilayer depth and mainly hexagonal shape. The trench surface structure is largely like that of the disordered '1 × 1' phase of the Si(111)-7 × 7 ↔ '1 × 1' phase transition and comprises mostly disordered Si adatoms with small ordered patches of (11 × 11), (9 × 9), c(5 × √5), c(4 × 4) and (2 × 2) structures along with some Co-ring clusters. This disordered '1 × 1' structure within the trench has formed at 600 °C, the growth temperature of $CoSi_2$ in reactive deposition epitaxy, much below the order–disorder phase transition temperature on Si(111)–(7 × 7). The structure around the trench remains (7 × 7). Electronically the trench is semiconducting. The surrounding 7 × 7 structure being metallic, the island–trench structure forms a lateral metal–semiconductor–metal structure.

© 2013 Published by Elsevier B.V.

1. Introduction

Growth of metal silicides on single crystal Si surfaces has been extensively studied for their importance in fundamental surface science research and possible applications in nanoelectronic devices [1–4]. Metal silicides are an integral part of microelectronics. Their usefulness comes from the chemically and structurally robust silicide/silicon interfaces and the tunability of the Schottky barrier height via choice of the silicide material [5,6]. For nanoelectronics it is important to understand the silicide/silicon systems in the nanoscale. Cobalt disilicide ($CoSi_2$) growth on silicon is important due to its thermal stability (up to ~900 °C) and its application as infrared detector [7,8], high speed transistor [9], low resistivity interconnect and contact material in sub-hundred nanometer device fabrication [10,11]. Growth of epitaxial and endotaxial self-organized cobalt silicide nanostructures on Si substrates of various crystallographic orientations is of tremendous current interest [12,13] and new phenomena in self-organized growth are still being discovered [13]. Here, we report on the epitaxial growth of self-organized $CoSi_2$ nanoislands on Si(111), which occurs via a trench formation around the islands. Although some trench–island structures were earlier observed for manganese silicide [14,15], cesium silicide [16] and iron silicide [17] growth on Si, no details of these structures have been investigated. Here, we present a detailed study of the trench–island structure regarding the trench-shape, relative trench edge energies, relation between trench volume and island volume, and geometrical and electronic structure within as well as outside the trench.

Trenches or vacancy islands on surfaces have been used to study many different kinds of phenomena. Vacancy island formation on various metal (Ag, Pt, Cr, Cu) surfaces has been extensively investigated [18–24]. Vacancy islands have been obtained via many different processes. Simultaneous growth of Ag adatom island and vacancy island on Ag(111) by modification of substrate surface using a vibrating scanning tunneling microscope tip has been investigated by Freund et al. [18]. The structure of the trench edges has been related to step formation energy. Vacancy islands have been formed via etching or sublimation of Cr atoms from a Cr(001) surface [19]. In this work the authors have investigated the morphological evolution of the surface as the atoms are removed. On the Pt(111) surfaces, vacancy islands have been formed by ion sputtering [20]. These authors have investigated the equilibrium shape of the trenches and determined the relative step free energies of different types of steps determining the trench morphology. Monatomic layer deep vacancy formation was observed on Cu(111) surfaces by depositing submonolayer quantities of Co [21,22], Fe [23] and Cr [24]. Quantum states of a two dimensional electron gas confined in a monolayer deep hexagonal trench have been investigated in Ref. [21]. Although most of the investigations on trench are on metal surfaces, there are some cases involving semiconductors (Si). Trenches (voids) were created in Si by He ion implantation followed by thermal annealing in order to investigate equilibrium crystal shape [25]. On a Si(111)-7 × 7 surface bilayer deep trenches were fabricated using a scanning tunneling microscope [26]. For silicide growth on Si, formation of trenches of irregular shapes has been observed for manganese silicide, cesium silicide and iron silicide growth [14–17]. We observe trench formation on Si(111)-7 × 7 surfaces and

* Corresponding author.
E-mail address: msbnd@iacs.res.in (B.N. Dev).
[1] Present address: Microelectronic Research Center, The University of Texas at Austin, Austin, TX 78758, USA.

0039-6028/$ – see front matter © 2013 Published by Elsevier B.V.
http://dx.doi.org/10.1016/j.susc.2013.10.006

concomitant growth of $CoSi_2$ islands inside the trench upon cobalt deposition at 600 °C. In earlier cases of silicide growth on Si, where trench–island structures were observed, no details of these structures were investigated. We have investigated several interesting aspects of trench–island structures. The trenches have predominant shapes guided by the substrate symmetry. Trench on the Si surface is created due to loss of Si atoms from the topmost bilayer of the Si(111) surface. These Si atoms have been consumed in the growth of $CoSi_2$ islands around which the trench is formed. Beyond the trench the Si(111) surface remains (7 × 7) reconstructed, like the original Si(111)-7 × 7 surface before Co deposition. The exposed surface within the trench is composed mostly of disordered Si adatoms along with small patches of ordered Si(111)-(9 × 9), -(11 × 11), -c(5 × √5), -c(4 × 4) and -(2 × 2) structures. Interestingly, these features are similar to the disordered high temperature '1 × 1' phase of the 7 × 7 ↔ '1 × 1' phase transition on the Si(111)-7 × 7 surfaces [27]. The trench also appears to have some cobalt-reacted ring clusters [28,29]. We also compare the electronic structure within the trench and on the $CoSi_2$ islands.

2. Experimental

Clean Si(111)-(7 × 7) surfaces were prepared from phosphorus doped (10–20 Ω-cm), oriented (within 0° ± 0.5°) Si(111) wafers. The substrate was degassed by heating it for 12–14 h at ~700 °C and then flashing at ~1250 °C for 1 min under ultrahigh vacuum (UHV) condition. This process produces a clean Si(111)-7×7 surface. The base pressure in the UHV chamber was 5×10^{-10} mbar. Epitaxial $CoSi_2$ nanostructures were grown on the atomically clean Si(111)–(7 × 7) surface by depositing 0.5 monolayer (ML) cobalt from a Knudsen cell onto the heated (600 °C) silicon substrate. Here, one monolayer of Co is equivalent to the atomic density on an ideal Si(111) surface (7.84×10^{14} atoms/cm^2). The Co deposition rate was 0.38 ML/min. The deposited amount of Co was determined in situ with a quartz crystal microbalance thickness monitor. A 1.5 Amp direct current was passed through the substrate for 15 min before Co deposition to achieve the substrate temperature. The substrate was maintained at the same temperature for another 10 min following Co deposition. Then the sample was allowed to cool down to room temperature (RT) before scanning tunneling microscopy (STM) measurements were made. The sample was transferred in situ from the growth chamber to the STM chamber (3×10^{-10} mbar). All the images were recorded with a scanning tunneling microscope (Omicron Nanotechnology) in situ at RT in the constant current mode.

3. Results

3.1. The trench–island structure

When Co is deposited on atomically clean heated Si(111)-7 × 7 surface or on Si surfaces with other orientations at 600 °C, $CoSi_2$ is formed [30]. While epitaxial $CoSi_2$ islands grow endotaxially (into the substrate) on Si(100) and Si(110) surfaces, on Si(111) surfaces they grow on top of the flat surface [13,31,32]. The islands are predominantly triangular because of the threefold symmetry of the Si(111) surface. The islands which grow near the surface step edges do not create trenches around them, as seen in Fig. 1. This feature was also observed earlier for manganese silicide [15] and in our earlier investigation on cobalt silicide [32] growth on Si(111). The step edges apparently act as the source of required Si for silicide island growth. This type of islands without a surrounding trench is abundant. Additionally, we find that $CoSi_2$ islands away from the step edges grow with a trench around them, although their number is small. Such $CoSi_2$ islands with a surrounding trench are shown in Fig. 2. In Ref. [15], for manganese silicide growth on Si, it was also observed that islands, which grow on a flat terrace away from surface steps, tend to have a trench around them. However in that work, unlike our case, the shape of the trenches was irregular. In the present case, as no trenches were present on the

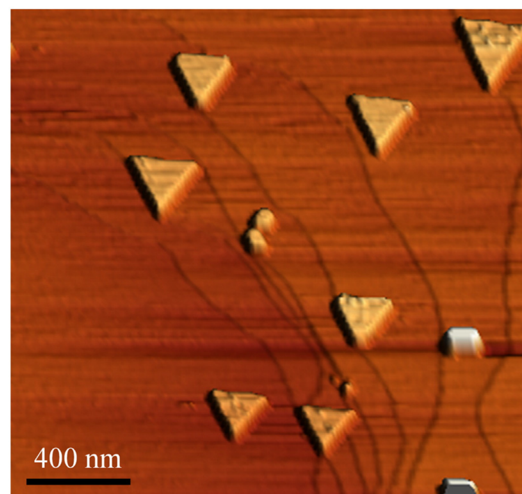

Fig. 1. Three dimensional view of a STM image (sample bias, $V_g = -1.9$ V, tunneling current, $I_t = 0.1$ nA) showing cobalt disilicide islands near the step edges on a Si(111) surface.

clean Si(111)-7 × 7 surface before Co deposition, it is clear that these trenches grow during silicide island formation. These trenches are typically 400–500 nm wide and 0.31 nm deep [equivalent to (111) planar spacing or removal of one bilayer Si]. The missing Si atoms from this trench region are apparently consumed in the growth of the $CoSi_2$ island inside the trench. Fig. 2(a), (b) and (c) shows STM images of island growth with a surrounding trench with three different island–trench structures. Islands are triangular and/or truncated triangular in shape whereas the trenches are hexagonal or partially rounded hexagonal shaped. The truncated $CoSi_2$ triangular island edges are parallel to the edges of the hexagonal trench. [In Fig. 2(c), we notice two intruding islands from the left side into the trench. There is an atomic step (not seen in the figure) present on the left side at ~320 nm from the left edge of the trench. So the intruding islands are a part of step–island structures like those in Fig. 1.]

Let us now discuss the shapes of islands and trenches. There are several theoretical studies on the shapes of islands and vacancy islands (or only trenches) on substrates of threefold symmetry [33,34]. The Si(111) surface possesses threefold symmetry. The growing $CoSi_2$ islands follow the substrate symmetry. So the formation of equilateral triangle shaped islands is quite natural. By Kinetic Monte Carlo simulation, Michely et al. [33] and Liu et al. [34] have found formation of different shapes of islands, including triangular and hexagonal on a surface of threefold symmetry. As shown and clarified in Ref. [33,34], the hexagonal islands on fcc(111) surfaces have two types of edges. The competition of advancement rate of these two types of edges would finally determine the shape of the island. When one type of edge advances faster than the other one, we are left with triangular hexagon shape. In the opposite case, we get an inverted triangular hexagon. If both edges compete equally the island attains an equilateral hexagon shape. The substrate symmetry serves to dictate not only the island shape but also the shape of the trench during the substrate etching. These shapes are seen in our island–trench combined structures. The shape of two-dimensional trenches or vacancy islands has also been investigated on a surface of threefold symmetry [Pt(111) surface] [20]. Experimentally the authors in Ref. [20] have found hexagonal shapes with unequal lengths of adjacent sides, similar to that in Fig. 2(c). Theoretically they have found that with increasing temperature the edges become rounded. However, in experiment, even at a given temperature, they have observed variations in shape [20,33,35], many of those are like the shapes in Fig. 2(a), (b) and (c). Although this kind of trench shapes has been observed on metal (111) surfaces, to our knowledge, there is no report on their observation on Si(111) surfaces.

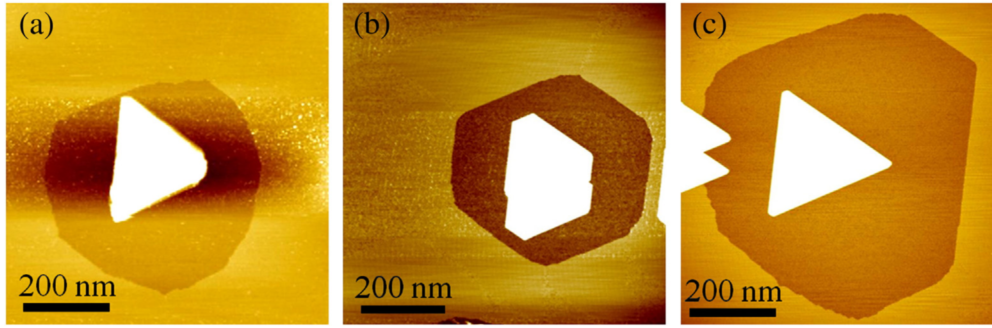

Fig. 2. STM images ($V_g = 1.9$ V, $I_t = 0.2$ nA) (a, b and c) show islands with different shapes of surroundings trenches.

The trench around the island is only a Si bilayer deep. From the STM images we have estimated the volume of the trenches and the corresponding islands. From these volumes we have determined the number of missing Si atoms within the trench (N^T_{Si}) and the number of Si atoms in the $CoSi_2$ islands (N^I_{Si}) for individual trench–island structures. We have determined the number of silicon atoms in the islands from the known number density of Si in $CoSi_2$. The number of silicon atoms depleted from the trench is calculated from the surface atomic density of Si an a Si(111) surface, i.e. 7.84×10^{14} atoms/cm^2, multiplied by 2 (because the depth of the trench is equivalent to two atomic layers). A plot of these results is shown in Fig. 3. The average number of excess Si atoms in the islands is ~$(1.6 \pm 0.3) \times 10^6$. With an average island area of ~0.03 μm^2, this amounts to a thickness of ~(1.0 ± 0.2) nm of $CoSi_2$. This can be interpreted as the thickness of the $CoSi_2$ island before the trench begins to form, assuming that the whole island area has developed before trench formation began. In Fig. 3 each point indicates one island. Islands with a surrounding trench are very few. There are islands, which extend from the trench to the surrounding terrace area. This happens when there are steps close to the trench. These islands cannot be included in this analysis. The result from the analysis presented in this paragraph should be considered as a preliminary estimate, as the data set is very small.

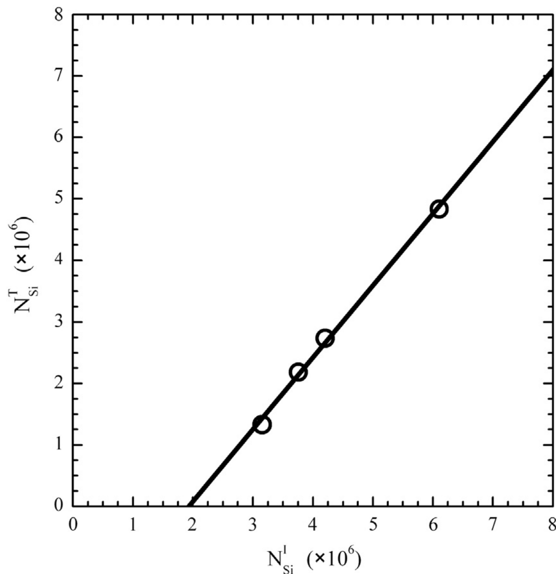

Fig. 3. The number of Si atoms missing in the trench (N^T_{Si}) is plotted against the number of Si atoms in the silicide island (N^I_{Si}) within the trench. The data points are fitted and extrapolated and the initial island height before the trench formation has been calculated.

From the height profiles across the island edges we have determined the facets of these $CoSi_2$ islands. Measurement of the inclination of the facets of $CoSi_2$ islands by STM has been used to identify the facet orientation. These are (131), (221), (311), (212), (113) and (122) crystallographic planes of $CoSi_2$; they are all low energy facets of $CoSi_2$. The $CoSi_2$ islands are expected to be in registry with the underlying Si substrate. However, this aspect can also be directly established by ion channeling experiments [36,37]. We will discuss the atomic structure within as well as outside the trench latter.

We now analyze the shape of the trenches in more details. We show the trench–island structure of Fig. 2(c) again in Fig. 4(a) with a straight-edge approximated outline of trench edges. Crystallographic directions ([10-1], [-12-1] and [-1-12]) on the (111) surface are shown by arrows in Fig. 4(a). Ignoring the small deviations, the edges of the trenches are all along <110> directions [see also Fig. 2(b)]. The island edges are also aligned along <110> directions. There are two types of edges, A-type and B-type on Si(111). A and B types of edges have different environments of surrounding atoms as for islands and trenches on (111) surfaces of fcc metals (Pt, Au, Ag) [18,20,38,39]. A B-type edge forms a {111} microfacet, while an A-type edge forms a {100} microfacet marked by a triangle and a rectangle, respectively in Fig. 4(c). Thus, a B-type edge would have lower free energy per unit length compared to an A-type edge as observed for the monolayer deep trenches on fcc metal surfaces. The longer length of the B-type edges in Fig. 4(a) is consistent with its lower free energy. The relative free energies per unit length of these edges can be calculated from the ratio of their length (l_A and l_B) or from the ratio of their distances from the center (r_A and r_B) via Wulff construction [40], when the shape is equilibrium. From Fig. 4(a, c), we see that $l_B > l_A$. This relationship also holds for the trench in Fig. 2(b). While it is evident from $l_B > l_A$ that the B-type edge has lower energy, the exact energy relationship between A- and B-type edges can only be determined from the equilibrium shape. To our knowledge for Si, this relationship is not yet known, although it is known for several fcc metal surfaces. However, for the two low energy facets {100} and {111} in the equilibrium crystal shape (or void shape) of Si, the ratio of free energies $\gamma_{100}/\gamma_{111} = 1.1$ [25]. From this it would be expected that the <110>/{111} B-type edge has lower energy than the <110>/{100} A-type edge. In Fig. 2(a), the edges are more rounded. Formation of kinks, as shown in Fig. 4(b), appears to be responsible for rounding of trench edges. Even on the equilibrium shape there can be kink motion leading to perimeter equilibrium fluctuations [20].

The etching of the bilayer deep Si produces trenches, which are most often with straight or slightly curved edges. A boundary region of the trench and the flat substrate terrace [the marked rectangular region in Fig. 4(a)] is shown in the STM image in Fig. 4(b) (200 × 200 nm^2) and in the inset of Fig. 4(b) (30 × 40 nm^2). From Fig. 4(b) it is clear that the flat terrace has preserved the Si(111)-7 × 7 surface. We notice that the non-straight edges of the trench have kink formation on the edge and that the etching of the trench proceeds by removing Si atoms in

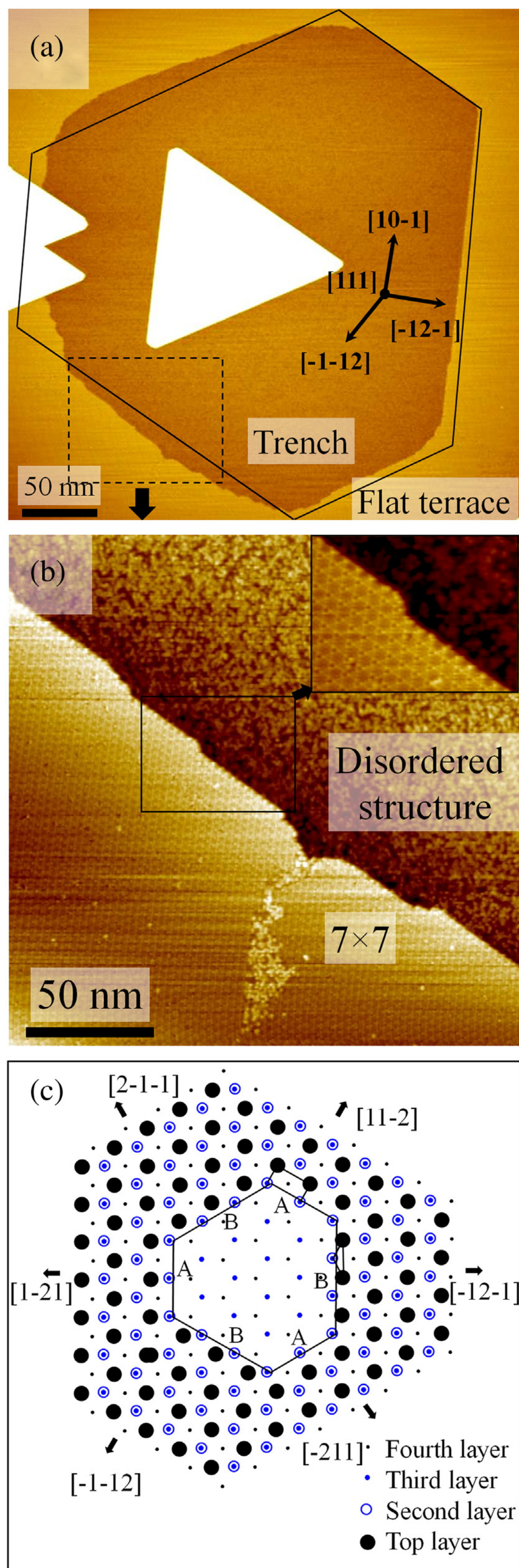

Fig. 4. (a) The STM image of Fig. 2(c) with a hexagon of threefold symmetry marked on it. The boxed part in (a) containing one boundary of the trench and the flat substrate terrace is shown in (b). The boxed part of (b) is enlarged and shown in the inset. From the inset it is clear that the flat terrace has preserved mostly the Si(111)-7 × 7 structure; however, the structure within the terrace is disordered. (c) Schematic model of the trench showing two types (A and B) of trench edges. Although the surface outside the trench is 7 × 7, for simplicity 1 × 1 structure is shown in (c); however, it illustrates the correct nature of the edges.

units of (7 × 7) unit cells or a row of (7 × 7) unit cells. These features are clearly seen in the inset of Fig. 4(b).

3.2. Structure within the trench

We now discuss the atomic structure within the trench. Although trenches around manganese silicide islands were observed in Ref. [14], the authors did not investigate the atomic structure within the trench. Here we investigate the surface structure within trenches around cobalt disilicide islands. The areas outside the trench show a Si(111)-(7 × 7) structure. This indicates that uniformly deposited Co atoms in these areas have diffused away from these areas and have been consumed into the growing $CoSi_2$ islands wherever they have nucleated. Missing Si atoms from the trench area have also been consumed in the growing

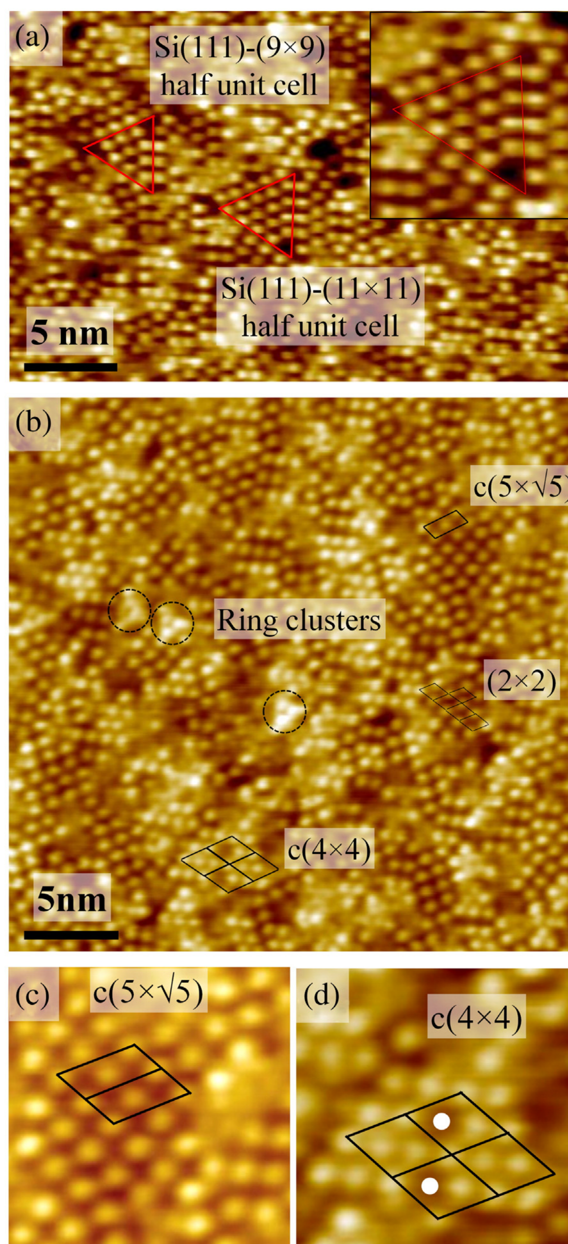

Fig. 5. STM images ($V_g = 1.9$ V, $I_t = 0.1$ nA) (a–d) show structures within the trench. Two half unit-cells of Si(111)-9 × 9, Si(111)-11 × 11 are seen in (a). Both of the half unit cells have one missing adatom; the (11 × 11) half unit cell is shown enlarged in the inset. (b) shows patches of Si(111)-c(5 × √5), c(4 × 4), and (2 × 2) adatom structures and encircled Si- or Co-ring clusters. (c) and (d) show the magnified images with c(5 × √5) and c(4 × 4) structures, respectively. In (d) two adatom vacancies are marked by two white circles.

$CoSi_2$ island within the trench. The surface within the trench shows several interesting structures. They are neither ordered (7 × 7) reconstructed surface, nor apparently completely free from Co. We have carried out STM measurements on different areas inside the trench as well as outside. The surface of the trench shows mostly disordered Si adatoms with some short range orders of adatom arrays with metastable reconstructions along with (possibly) some cobalt ring clusters. Fig. 5(a) and (b) shows atomically resolved STM images within the trench. Disordered Si(111) surface usually shows such features [27]. Fig. 5(a) shows two half unit cells, marked by triangles, of Si(111)-(11 × 11) and Si(111)-(9 × 9) reconstruction. (Each half unit cell has a missing adatom). The enlarged 11 × 11 half unit cell is shown in the inset of Fig. 5(a). This half unit cell should contain 15 Si adatoms. With one missing adatom, it contains only 14 Si adatoms. Fig. 5(b) shows another region within the trench. In Fig. 5(b) a small region shows Si(111)-c(5 × √5) structure and another region shows a c(4 × 4) structure. These regions are shown magnified in Fig. 5(c) and (d), respectively. Overall there are many small patches of 2 × 2 adatom structures. Fig. 5(b) also shows some circled structures, which are either Co ring clusters [28,29] or Si adatom ring clusters [32]. One of them is shown enlarged in the inset. A Co-ring cluster is a Co atom surrounded by six Si adatoms. Under the STM imaging condition (empty state, $V_g = +1.9$ V, $I_t = 0.2$ nA) used here, they appear nearly triangular as observed in earlier studies for sub-monolayer Co deposition on a Si(111)-7 × 7 surface at RT followed by annealing at ~600 °C [28,29]. Under this imaging condition a Si-adatom ring cluster also looks like the triangular patterns in the encircled structures [32].

The overall trench region has similarity with the Si(111) disordered '1 × 1'structure as observed in the Si(111)-7 × 7 ↔ '1 × 1' phase transition [27]. That the trench surface is indeed a disordered '1 × 1' surface is revealed by taking fast Fourier transform (FFT) of STM images from the trench region and comparing them with FFTs of images from the terrace outside the trench. Fig. 6(a) shows the FFT of Fig. 5(b). It shows the underlying 1 × 1 pattern of the disordered surface. Fig. 6(b) shows the FFT from outside the trench which shows the 7 × 7 pattern. If a bilayer of Si atoms is removed from the Si(111)-7 × 7 surface to form a $CoSi_2$ island within a trench, the trench surface, if ordered would be a −7 × 7 reconstructed surface. Apparently, the etching of a bilayer of Si(111)-7 × 7 within the trench region leaves behind a surface where the Si adatoms are disordered with some small patches of locally ordered regions. A disordered surface has also been observed in trenches related to $FeSi_2$ growth on Si(111)-7 × 7 surfaces [17]. However, no detailed investigation has been made. The disordered surface of the trench is likely to be metastable as the sample was kept at the deposition temperature for just 10 min following Co deposition. In a related earlier study [32], we captured some '1 × 1' disordered regions on a Si(111) surface by quenching it to room temperature from near the (7 × 7) ↔ '1 × 1' phase transition point. Prolonged annealing at 600 °C transformed the disordered '1 × 1' surface to a (7 × 7) reconstructed surface. However, in the present case, even, longer annealing may not convert the surface fully to a (7 × 7) structure. If the ring clusters, observed here [in Fig. 5(b)], are Co-induced as in Ref. [28], those regions will not be converted to a (7 × 7) structure. However, if they are Si adatom ring clusters as in Ref. [32], they will be converted to a (7 × 7) structure upon prolonged annealing.

3.3. Electronic structure

The results of scanning tunneling spectroscopy (STS), i.e. current (I) vs voltage (V) (with set point i.e. $V_g = -1.9$ V and $I_t = 0.2$ nA), measurements on the flat top $CoSi_2$ islands and on the trench surface [in regions as in Fig. 5(a) or (b)] have been plotted in Fig. 7(a). Each plot is an average of about ten data sets obtained from different locations. The electronic density of states (DOS) is proportional to (dI/dV)/(I/V), which has been obtained from numerical derivative of the I–V curves. The (dI/dV)/(I/V) vs V plots for measurements on top of the $CoSi_2$ islands and within the trenches are shown in Fig. 7(b). In the filled state (valence band) DOS of $CoSi_2$ islands, the main peaks are at around −0.9 eV and −2.1 eV. This is in good agreement with previous experiments [41,42] and theory [41–43]. From Fig. 5(a) and (b) we notice that the trench surface contains mainly Si adatoms. DOS from adatoms plus rest atoms on a Si(111) surface has very similar features [44] to the observed STS results in Fig. 7(b) from the trench surface. The STS results [Fig. 7(b)] obtained from the trench area show also good agreement with the results of Odagiri et al. [29], who made measurements on selected Si adatoms and Co atoms of Co-ring clusters. DOS on Co atoms and on two types of Si adatoms around the Co atom in the Co-ring clusters has very small differences. So, the observed STS results are consistent with the structures observed in the STM images. It is known that the Si(111)-7 × 7 surface has a metallic character [45–48]. The disordered Si '1 × 1' surface within the trench is semiconducting. This semiconducting behavior is revealed in the I–V plot shown in the semi-log plot in Fig. 8(a). Data taken from different locations on the '1 × 1' surface show similar results. Fig. 8(a) shows the average of results from measurements on seven different locations. For comparison, the metallic nature of the 7 × 7 region is also shown in Fig. 8(b). With the metallic $CoSi_2$ island the island–trench structure with its surrounding (7 × 7) area forms a lateral metal–semiconductor–metal structure.

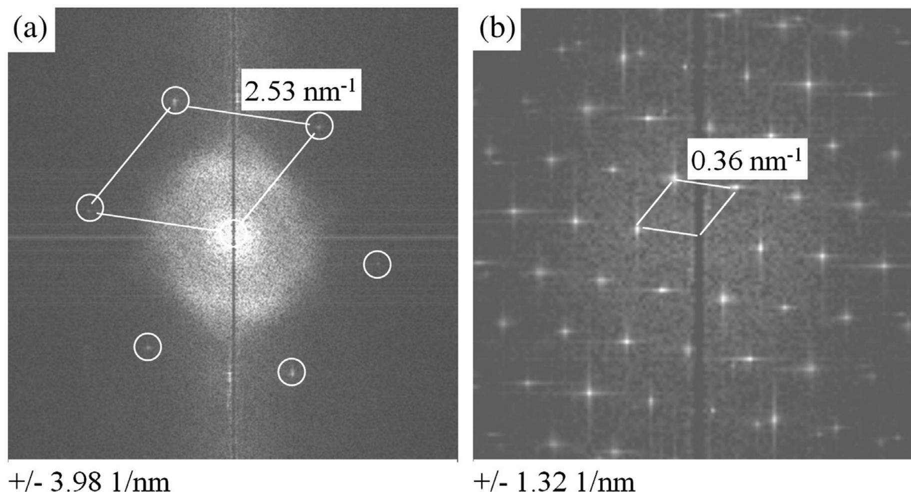

Fig. 6. The fast Fourier transform of STM images from (a) the trench surface and (b) a Si(111)-7 × 7 region. In (a) reciprocal lattice points are encircled.

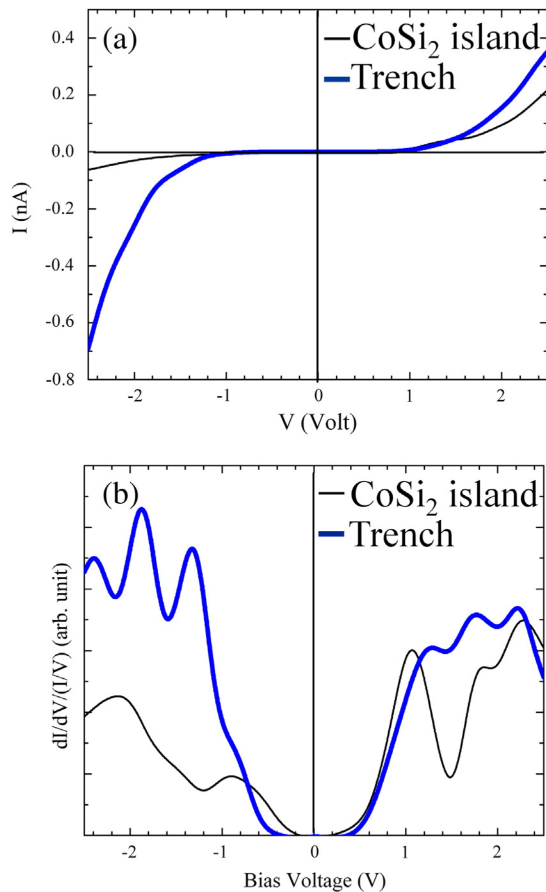

Fig. 7. Scanning tunneling spectroscopy (STS) (tunneling current–voltage) results from measurements carried out on the top surface of $CoSi_2$ islands and on the trench surface on regions like those in Fig. 5(a), (b).

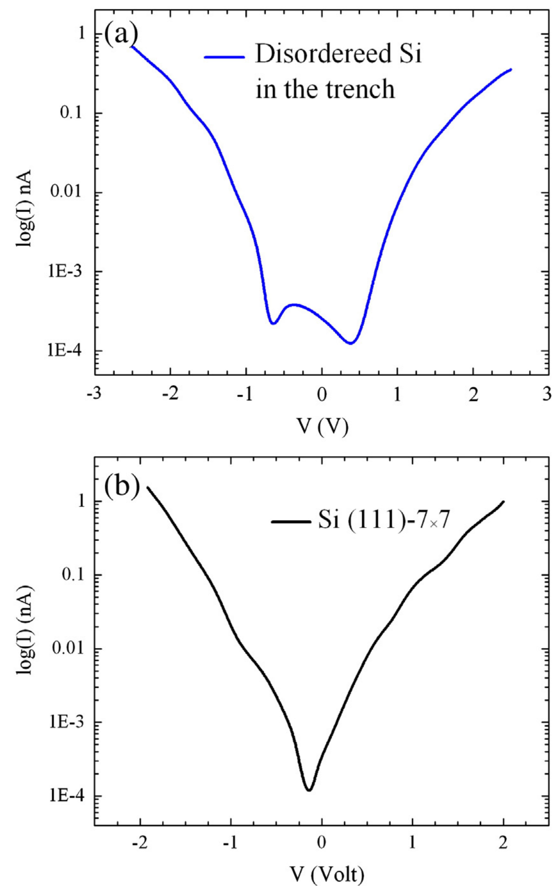

Fig. 8. The plot in (a) shows the semi-log tunneling current (I) vs voltage (V) on the trench surface. A band gap of ~1.1 V is seen. The plot in (b) shows the semi-log tunneling current (I) vs voltage (V) on the Si(111)-7 × 7 surface.

4. Summary and conclusions

In conclusion, we have observed trench–island structures in the self-organized growth of $CoSi_2$ nanostructures on Si(111) surfaces. In the trench–island structure, $CoSi_2$ islands are surrounded by trenches. The islands are triangular or hexagonal. The trenches are predominantly of hexagonal shape, some with rounded edges. Adjacent sides of the hexagon are two types of edges with different free energies. The B-type <110>/{111} edges apparently have lower energies compared to the A-type <110>/{100} edges. The atomic structure within the trench is very similar to that of the disordered '1 × 1' phase of the 7 × 7 ↔ '1 × 1' phase transition that occurs on Si(111) around 870 °C. Diffusion of Si from the trench region into the growing $CoSi_2$ island has apparently left the exposed trench surface disordered. The trench surface is composed mainly of disordered Si adatoms along with some small patches of Si(111)-(11 × 11), -(9 × 9); -c(5 × √5), -c(4 × 4) and -(2 × 2) reconstructions and possibly some Co-ring clusters. To our knowledge the c(5 × √5) phase on a disordered Si(111) surface was not reported earlier. The trench region is semiconducting. The trench–island structure, along with its surrounding metallic (7 × 7) structure, forms a lateral metal–semiconductor–metal structure with possible nanoscale device applications.

Acknowledgment

Jagadish Ch Mahato and Debolina Das are supported by a CSIR Fellowship [09/080(0674)/2009-EMR-I] and [09/080(0725)/2010-EMR-I] respectively. The work is partially supported by the IBIQuS project.

References

[1] L.J. Chen, Silicide Technology for Integrated Circuits, The Institute of Engineering and Technology, London, UK, 2009.
[2] Y. Wu, J. Xiang, C. Yang, W. Lu, C.M. Lieber, Nature (London) 430 (2004) 61.
[3] H.C. Hsu, W.W. Wu, H.F. Hsu, L.J. Chen, Nano Lett. 7 (2007) 885.
[4] Z. Zhang, L.M. Wong, H.G. Ong, X.J. Wang, J.L. Wang, S.J. Wang, H.Y. Chen, T. Wu, Nano Lett. 8 (2008) 3205.
[5] K.N. Tu, J.W. Mayer, in: J.M. Poate, K.N. Tu, J.W. Mayer (Eds.), Thin Films -Interdiffus. React, John Wiley, 1978, p. 359.
[6] A.H. Reader, A.H. Ommen, P.J.W. Weijs, R.A.M. Wolters, D.J. Oostra, Rep. Prog. Phys. 56 (1993) 1397.
[7] R.W. Fathauer, A. Ksendzov, J.M. Ionnally, T. George, Phys. Rev. B 44 (1991) 1345.
[8] R.W. Fathauer, J.M. Ionnally, C.W. Nieh, S. Hashimoto, Appl. Phys. Lett. 57 (1990) 1419.
[9] J.C. Hensel, A.F.J. Levi, R.T. Tung, J.M. Gibson, Appl. Phys. Lett. 47 (1985) 151.
[10] S.P. Murarka, Intermetallics 3 (1995) 173.
[11] S. Vaidya, R.J. Schutz, A.K. Sinha, J. Appl. Phys. 55 (1984) 3514.
[12] Z. He, D.J. Smith, P.A. Bennett, Phys. Rev. Lett. 93 (2004) 256102.
[13] J.C. Mahato, Debolina Das, R.R. Juluri, R. Batabyal, Anupam Roy, P.V. Satyam, B.N. Dev, Appl. Phys. Lett. 100 (2012) 263117.
[14] Z. Zou, W. Li, J. Liang, D. Wang, Acta Mater. 59 (2011) 7473.
[15] Z.Q. Zou, H. Wang, D. Wang, Q.K. Wang, J.J. Mao, X.-Y. Kong, Appl. Phys. Lett. 90 (2007) 133111.
[16] D. Lee, S.M. Jeon, G. Lee, S. Kim, C. Hwang, H. Lee, Surf. Sci. 601 (2007) 3823.
[17] M. Krause, F. Blobner, L. Hammer, K. Heinz, U. Starke, Phys. Rev. B 68 (2003) 125306.
[18] J.E. Freund, M. Edelwirth, J. Grimminger, R. Schloderer, W.M. Heckl, Appl. Phys. A 66 (1998) S787.
[19] S.J. Tang, S. Kodambaka, W. Swiech, I. Petrov, C.P. Flynn, T.C. Chiang, Phys. Rev. Lett. 96 (2006) 126106.
[20] J. Ikonomov, K. Starbova, H. Ibach, M. Giesen, Phys. Rev. B 75 (2007) 245411.
[21] L. Niebergall, G. Rodary, H.F. Ding, D. Sander, V.S. Stepanyuk, P. Bruno, J. Kirschner, Phys. Rev. B 74 (2006) 195436.
[22] J. Figuera, J.E. Prieto, C. Ocal, R. Miranda, Surf. Sci. 307–309 (1994) 538.
[23] A. Brodde, K. Dreps, J. Binder, Ch. Luau, H. Neddermeyer, Phys. Rev. B 47 (1993) 6609.
[24] J.K. Yoon, G. Jung, H. Kim, K.H. Chung, S. Kahng, Thin Solid Films 519 (2011) 1375.
[25] D.J. Eaglesham, A.E. White, L.C. Feldman, N. Moriya, D.C. Jacobson, Phys. Rev. Lett. 70 (1993) 1643.

[26] A. Kraus, S. Hildebrandt, R. Kulla, G. Wilhelmi, H. Neddermeyer, Appl. Phys. A 66 (1998) S953.
[27] Y.N. Yang, E.D. Williams, Phys. Rev. Lett. 72 (1994) 1862(and the reference therein).
[28] P.A. Bennett, M. Copel, D. Cahill, J. Falta, R.M. Tromp, Phys. Rev. Lett. 69 (1992) 1224.
[29] M. Odagiri, I. Mochizuki, Y. Shigeta, A. Tosaka, Appl. Phys. Lett. 97 (2010) 151911.
[30] R.T. Tung, J.C. Bean, J.M. Gibson, J.M. Poate, D.C. Jacobson, Appl. Phys. Lett. 40 (1982) 684.
[31] P.A. Bennett, Zhian He, David J. Smith, F.M. Ross, Thin Solid Films 519 (2011) 8434.
[32] J.C. Mahato, D. Das, A. Roy, R. Batabyal, R.R. Juluri, P.V. Satyam, B.N. Dev, Thin Solid Films 534 (2013) 296.
[33] T. Michely, M. Hohage, M. Bott, G. Comsa, Phys. Rev. Lett. 70 (1993) 3943.
[34] S. Liu, Z. Zhang, G. Comsa, H. Metiu, Phys. Rev. Lett. 71 (1993) 2967.
[35] S. Chakraborty, J. Kamila, B. Rout, B. Satpati, P.V. Satyam, B. Sundaravel, B.N. Dev, Surf. Sci. 549 (2004) 149.
[36] P.V. Satyam, K. Sekar, G. Kuri, B. Sundaravel, D.P. Mahapatra, B.N. Dev, Appl. Surf. Sci. 125 (1998) 173.
[37] P.V. Sataym, K. Sekar, G. Kuri, B. Sundaravel, D.P. Mahapatra, B.N. Dev, Philos. Mag. Lett. 73 (1996) 309.
[38] T. Michely, G. Comsa, Surf. Sci. 256 (1991) 217.
[39] T. Michely, K.H. Besocke, G. Comsa, Surf. Sci. Lett. 230 (1990) L135.
[40] C. Herring, Phys. Rev. 82 (1951) 87.
[41] C. Pirri, J.C. Peruchetti, G. Gewinner, J. Derrien, Phys. Rev. B 30 (1984) 6227.
[42] E. Belint, C. Senemaudt, L. Martinage, J.Y. Veuillen, D.A. Papaconstantopoulos, A. Pasture, F. Cyrot-Lackmann, J. Phys. Condens. Matter 2 (1990) 3247.
[43] T. He, H. Zhang, Z. Wang, X. Zhang, Z. Xi, X. Liu, M. Zhao, Y. Xia, L. Mei, Phys. E. 41 (2009) 1795.
[44] R.J. Hamers, R.M. Tromp, J.E. Demuth, Phys. Rev. Lett. 56 (1986) 1972.
[45] R.J. Hamers, R.M. Tromp, J.E. Demuth, Surf. Sci. 181 (1987) 346.
[46] J. Ortega, F. Flores, R. Perez, A.L. Yeyati, Prog. Appl. Surf. Sci 59 (1998) 233.
[47] J.E. Demuth, B.N.J. Persson, A.J. Schell-Sorokin, Phys. Rev. Lett. 51 (1983) 2214.
[48] P. Martensson, W.-X. Ni, G.V. Hansson, J.M. Nicholls, B. Riehl, Phys. Rev. B 36 (1987) 5974.